Blast Wave Transmission In Full-Scale Multi-Node Tunnel Networks: Interaction Regimes, Wave Recompression, And Scaling Deviation

Cheng-Wei Hung[1], Sheng-Jung Pi[2], and Pen-Chou Chen[3*]

[1] *Department of Civil Engineering and Environmental Informatics, Minghsin University of Science and Technology, Hsinchu 30401, Taiwan*
[2] *National Defense University, Chung Cheng Institute of Technology, School of National Defense Science, Taoyuan 33551, Taiwan*
[3] *Department of Civil Engineering, National Chung Hsing University, Taichung 40227, Taiwan*
[*] *Corresponding author. E-mail: s883309kimo@gmail.com*

Received: April 04, 2026; Accepted: April 13, 2026

Blast-wave transmission in underground tunnel systems is strongly affected by sequential geometric discontinuities, yet most previous studies have focused on isolated tunnel components or short-distance propagation. This study investigates pressure transmission behavior in a 100 m full-scale multi-node tunnel network subjected to near-field external detonation. The network contains elbows, branching junctions, and cross-sectional transitions, representing a realistic underground protective access system. Numerical simulations were conducted using a validated arbitrary Lagrangian–Eulerian blast-analysis framework for 10 kg, 100 kg, and 500 kg C-4 charges. The validation lineage of the numerical framework, together with the mesh-sensitivity basis adopted in the present model, is summarized explicitly in the Methods section.

To distinguish local geometric interaction from quasi-independent propagation, two spacing regimes were defined according to the hydraulic diameter of the tunnel. A Node Interaction Index (NII) was introduced to quantify the deviation between coupled multi-node transmission and independent attenuation prediction. The results show that closely spaced discontinuities produce wave recompression, extended positive-phase duration, and locally amplified peak pressure, whereas larger spacing leads to near-independent attenuation behavior. Comparison with conventional cube-root scaling further reveals a sustained deviation range in the full-scale tunnel network, indicating that classical similarity relations are conditionally valid in confined long-distance propagation. Across the three charge weights, the spatial pattern of interaction remains similar, while the persistence of impulse-related deviation becomes more pronounced as charge weight increases. The proposed interaction-aware framework provides a practical basis for blast-resistant assessment and design of underground protective tunnel systems.

Keywords: Blast wave transmission; Tunnel network; near-field explosion; Full-scale simulation; Geometric discontinuity; Wave recompression; Sscaling deviation; Protective structures

http://dx.doi.org/10.6180/jase.202609_32.024

1. Introduction

Underground tunnel systems are widely used in military command facilities, transportation infrastructures, and protective shelters because surrounding ground confinement can reduce direct blast effects on critical assets. However, when an external detonation occurs near a tunnel portal, the resulting shock wave may enter the tunnel and propagate through a sequence of bends, branches, and sectional transitions. In such cases, the internal pressure field is governed not only by free-field blast attenuation but also by confinement, repeated reflection, and geometry-induced

wave interaction [1–5]. Reliable prediction of blast transmission in complex tunnel systems is therefore essential for protective design and risk assessment.

Existing studies have provided valuable insights into blast propagation in straight tunnels, elbowed passages, T-junctions, and pressure-reduction devices. Nevertheless, most published results are based on isolated geometric components or reduced-scale laboratory configurations, and the findings are commonly interpreted using component-level attenuation factors [6–12]. Such approaches are useful for local analysis, but they do not fully represent the propagation behavior in full-scale underground networks where multiple geometric discontinuities occur in sequence and interact with each other.

The engineering problem addressed in this study is that conventional component-based attenuation logic is insufficient when a blast wave enters a full-scale underground tunnel network containing multiple sequential discontinuities. In such networks, the loading demand at a downstream node may be governed by residual reflections and inter-node coupling rather than by single-component attenuation alone. This gap motivates the present system-level investigation.

The present study focuses on blast-wave transmission in a 100 m full-scale underground tunnel network subjected to near-field external detonation. Unlike previous component-level studies, the emphasis here is placed on system-level propagation behavior, including the distinction between interaction-dominated and quasi-independent regimes, the physical mechanism of wave recompression, and the applicability limit of conventional cube-root scaling in confined long-distance propagation. This repositioning differentiates the present work from earlier studies on isolated tunnel bends, branching components, near-field mapping procedures, and pressure-reduction modules.

In this study, a geometric discontinuity denotes a local tunnel configuration change that modifies the blast-wave path, reflection condition, or effective confinement state. Typical examples include elbows, branching junctions, and cross-sectional transitions. When these discontinuities are closely spaced, reflected waves generated at an upstream node may overlap with the downstream incident front before sufficient dissipation occurs, producing local recompression and elevated peak pressure. To quantify this effect, a Node Interaction Index (NII) is introduced and used together with spacing-based regime classification.

The main objectives of this paper are therefore to: (1) characterize pressure attenuation and waveform evolution in a full-scale multi-node tunnel network; (2) identify the transition between interaction-dominated and quasi-independent propagation regimes; (3) quantify coupling intensity through the NII; and (4) evaluate the extent to which classical cube-root scaling deviates from full-scale confined propagation results. The resulting framework is intended for engineering assessment of blast-resistant underground tunnel systems.

The main contributions of this paper are summarized as follows:

- A full-scale 100 m multi-node tunnel-network framework is established to examine coupled blast-wave transmission beyond isolated component behavior.
- Spacing-based interaction regimes are interpreted using hydraulic-diameter normalization together with waveform and NII indicators rather than geometric description alone.
- An uncertainty-aware interpretation of the independent-node baseline is incorporated to clarify the robustness of the Node Interaction Index.
- A practical interaction-corrected scaling formulation is proposed for preliminary engineering assessment in confined multi-node tunnel networks.

Compared with previous studies that mainly addressed straight tunnels, isolated elbows, T-junctions, or pressure-reduction devices [6–11, 13–17], the present work emphasizes sequential interaction in a realistic full-scale network, identifies persistence of interaction across charge weights, and interprets the resulting deviation from conventional cube-root scaling.

Comparative positioning of representative prior studies and the present work.

2. Theory and formula

2.1. Characteristic length and spacing regimes

Because the investigated tunnel contains non-circular sections, the hydraulic diameter was adopted as the characteristic length scale:

$$D\_h = \frac{4A}{P} \tag{1}$$

where A is the tunnel cross-sectional area and P is the wetted perimeter. The hydraulic diameter provides a unified geometric measure for comparing spacing effects among sections that do not possess a single conventional diameter.

The spacing between adjacent discontinuities was normalized by D_h. Based on the present simulation dataset, spacing smaller than 5D_h consistently exhibited reflected-wave overlap, local recompression, and NII values greater than unity, whereas spacing larger than 12D_h approached

Study focus	Typical scope in prior work	Position of the present study
Straight/isolated tunnel components	Single tunnel segment or one local discontinuity	Sequentially coupled full-scale network with multiple discontinuities
Attenuation description	Component-level attenuation or local peak redistribution	System-level coupling, waveform broadening, and recompression persistence
Scaling interpretation	Local or reduced-scale interpretation	Full-scale confined propagation compared against cube-root baseline
Engineering outcome	Local mitigation insight	Interaction-aware assessment framework for network-level blast evaluation

quasi-independent attenuation behavior. These two thresholds are not claimed to be universal constants; rather, they serve as practical regime indicators derived from the present full-scale network.

The interval between 5D_h and 12D_h should be interpreted as a transition zone rather than as a sharp boundary. In this intermediate range, the response depends on residual wave strength, local geometric type, branch/turn arrangement, and charge weight, so spacing alone is insufficient for classification. In practical terms, the most influential controlling parameters in this transition band are the residual shock strength arriving from the upstream node, the local discontinuity family (elbow, branch, or cross-sectional change), and the associated reflection geometry.

In the present dataset, the lower threshold of 5D_h was selected as the spacing below which the screened node pairs consistently showed both NII >= 1.10 and an observable extension of positive-phase duration relative to the quasi-independent reference segments. The upper threshold of 12D_h was selected as the distance beyond which the post-processed curves approached NII $\approx$ 1.00-1.05 and the waveform returned to a single-front decay pattern. Accordingly, the two thresholds should be interpreted as data-derived engineering bounds for the current full-scale configuration rather than universal constants.

2.2. Node Interaction Index

To quantify the deviation between coupled multi-node transmission and independent-node prediction, the Node Interaction Index was defined as:

$$\mathrm{NII} = \frac{\mathrm{P\_\ coupled}}{\mathrm{P\_\ independent}} \tag{2}$$

where P_coupled is the peak pressure obtained from the coupled multi-node simulation and P_independent is the corresponding pressure predicted under an independent-transmission assumption. Values of NII > 1 indicate interaction-induced amplification, whereas values close to 1 indicate that quasi-independent attenuation is dominant.

In the present study, P_independent was calculated sequentially rather than inferred heuristically. First, a portal-entry pressure was obtained for each charge case from the validated near-field model. Next, independent attenuation factors were assigned to each local component family using previously validated component-level references: straight-tunnel/decompression transmission from Ref. [18] and tunnel-variation effects (elbow, T-junction, and branch-type path changes) from Ref. [19]. These factors were then multiplied sequentially along the propagation path to generate the independent prediction. Where the present full-scale geometry was not exactly identical to a previously validated component, the nearest validated component family was used as a reference approximation; accordingly, P_independent should be interpreted as a baseline decoupled estimate rather than an exact local predictor.

This definition is intentionally conservative: if adjacent discontinuities truly behave independently, the ratio should remain close to unity. Systematic deviations above unity therefore indicate that the independent-transmission assumption underestimates the coupled response because local reflections are still active when the wave reaches the next discontinuity.

To clarify the uncertainty of the independent-node prediction, the component-based attenuation factors were interpreted as baseline reference values and examined in a bounded sensitivity sense. For geometrically matched components, the original validated attenuation factors were retained; for partially mismatched full-scale geometries, the same component family was used as an approximation and the resulting NII values were interpreted together with waveform evidence rather than as a single deterministic indicator. This uncertainty-aware reading does not eliminate approximation error, but it prevents over-interpretation of P_independent and strengthens the reliability of the regime classification.

In addition to peak pressure, impulse was also evaluated because it reflects the integrated effect of waveform broadening and positive-phase duration. Both quantities were used to interpret interaction strength and scaling deviation along the propagation path.

2.3. Scaling-deviation assessment

To evaluate the applicability of conventional scaled-distance prediction in the full-scale tunnel network, the numerical results were compared with cube-root scaling-based predictions. The scaled reference values P_SC(x) and I_SC(x) were taken from free-field incident-blast relations based on the UFC 3-340-02/Kingery-Bulmash framework, expressed at equivalent scaled distance and then used as the baseline for comparison with the confined-network simulations. Two deviation ratios were adopted:

$$R\_P\ (x) = \frac{P\_FS(x)}{P\_SC(x)} \tag{3}$$

$$R\_I\ (x) = \frac{I\_FS(x)}{I\_SC(x)} \tag{4}$$

where P_FS(x) and I_FS(x) are the simulated full-scale peak pressure and impulse at distance x, and P_SC(x) and I_SC(x) are the corresponding scaled predictions. Values consistently above unity indicate that full-scale confined propagation produces higher demand than conventional scaling would suggest.

For preliminary engineering use, an interaction-corrected scaling form may be written as P_IC(x) = C_int(x) P_SC(x) and I_IC(x) = C_int,I(x) I_SC(x), where the correction factors are obtained from the envelope of the present full-scale results. For the current tunnel network, C_int(x) may be conservatively taken as 1.10-1.30 in the interaction-dominated deviation zone and about 1.00-1.10 outside that zone. This expression is not proposed as a universal law; instead, it provides a practical quantitative bridge between conventional scaling and the observed confined multi-node response.

3. Experimental setup

The investigated system is a 100 m full-scale underground tunnel network containing multiple sequential geometric discontinuities, including elbows, branching junctions, and cross-sectional transitions. The network is intended to represent a realistic underground protective access system rather than an isolated tunnel component. Monitoring nodes were distributed along the main propagation path to evaluate peak pressure, impulse, and waveform evolution.

The explosive charge was positioned outside the tunnel entrance to represent a near-field external detonation scenario. Three charge weights—10 kg, 100 kg, and 500 kg C-4—were considered in order to compare propagation behavior across different loading intensities. This loading definition is consistent with the near-field numerical framework adopted in the authors' earlier blast-model validation studies.

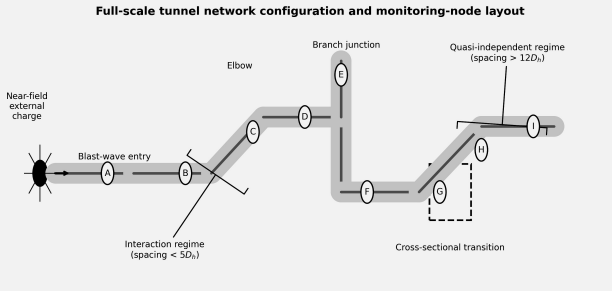

Fig. 1. Full-scale tunnel network configuration and monitoring-node layout, showing the interaction regime for closely spaced discontinuities and the quasi-independent regime for larger spacing.

3.1. Numerical analysis framework

The numerical framework used in the present study was not introduced as a de novo model. Instead, it follows a validated modeling lineage previously established by the authors for near-field blast loading, confined tunnel transmission, and tunnel-variation effects. In response to the review comments, the validation basis is summarized quantitatively in Table 1, including representative error levels or trend-matching evidence reported in the prior studies.

Table 1 shows that the present manuscript relies on an experimentally anchored numerical lineage rather than on an unverified standalone model. The current contribution is therefore the system-level interpretation of blast transmission in a full-scale multi-node network, whereas the underlying solver chain, loading representation, and component-scale transmission behavior were validated previously with experimentally or empirically benchmarked cases.

Blast-wave propagation was analyzed using a validated arbitrary Lagrangian–Eulerian (ALE) numerical framework. Based on the authors' prior near-field blast simulation work, LS-DYNA with mapping-assisted ALE treatment was adopted as the commercial hydrocode environment for the present full-scale tunnel analyses. The explosive was modeled using a Jones–Wilkins–Lee equation of state, and the air domain was represented by an ideal-gas formulation. The numerical strategy follows the same modeling lineage used in the authors' previously published near-field explosion and tunnel-transmission studies, but the present paper shifts the contribution from component-level validation to system-level network interpretation.

A mesh-sensitivity check was performed before the final analyses. Element sizes of 50 mm, 30 mm, and 20 mm were compared, and the difference in peak pressure between the

Table 1. Validation lineage of the numerical framework and its relevance to the present full-scale tunnel-network analysis.

Reference	Validated case	Evidence reported in prior work	Relevance to present study
[20]	Near-field free-air and nearsurface blast mapping	Free-air/near-surface mapping errors below 2% versus empirical blast relations; reflected-peak errors of -14.05% and +5.88% versus steel-plate tests.	Supports the ALE mapping strategy near-field external-detonation loading treatment used at the portal.
[18]	Straight tunnel and decompression module transmission	Most attenuation cases within 5.4% – 24% against tunnel experiments; one local outlier reached 46% in the most severe double-orifice case.	Supports the pressure transmission treatment inside confined tunnel passages and the use of attenuation as a response metric.
[19]	Tunnel variations including elbowed and branched paths	Component-scale tunnelvariation study reproduced measured path-dependent effects, including about 7% elbow attenuation, +7% Tjunction amplification, 22% branch-turn attenuation, and 37% straight-path attenuation; validation was trend-matching rather than a single error metric.	Supports the use of geometric-discontinuity effects and path-sensitive transmission logic in the present multi-node network.

30 mm and 20 mm meshes remained within 3%; therefore, the 30 mm mesh was adopted for the production analyses. Non-reflecting boundaries were used at the far-field air domain, the portal remained open to permit blast-wave entry, and the tunnel walls were treated consistently with the validated rigid-boundary transmission framework used in the reference tunnel studies. In the present paper, the emphasis is on pressure transmission within the air domain rather than structural damage to the lining.

The mesh-convergence check was evaluated at representative near-, intermediate-, and downstream monitoring locations. The 30 mm mesh reproduced the 20 mm mesh trend in both peak pressure and waveform shape, while the 50 mm mesh showed visibly coarser front resolution in the near-portal region. Because the peak-pressure difference between the 30 mm and 20 mm meshes remained within 3% and did not change the regime interpretation, the 30 mm discretization was adopted as the accuracy-efficiency compromise for the production analyses.

3.2. Evaluation nodes and metrics

Pressure histories were extracted at representative monitoring-node pairs to distinguish interaction-dominated and quasi-independent segments. Peak pressure, positive-phase impulse, and waveform shape were used as the primary response metrics. The selected node-pair categories are summarized in Table 2.

Table 2. Selected monitoring-node categories and spacing-based regime definitions.

Node pair	Normalized spacing	Regime classification
B-C	$< 5Dh$	Interaction-dominated
G-I	$> 12Dh$	Quasi-independent

4. Result discussions

4.1. Global attenuation trend in the 100 m tunnel network

The full-scale simulations show that peak pressure and impulse both decrease along the propagation path, but neither response can be represented by a single attenuation law over the entire 100 m network. Peak pressure drops rapidly in the near-portal region and then exhibits a sustained deviation band over the intermediate distance range, where the full-scale results remain above cube-root scaling predictions. Impulse follows a smoother overall decay trend, yet it also retains an extended deviation interval because waveform broadening and reflection accumulation continue to contribute to the integrated loading even after the initial pressure peak has attenuated.

The present system-level behavior is distinct from the attenuation patterns reported for isolated tunnel bends, straight segments, and pressure-reduction devices. In those component-scale studies, the main emphasis was on local pressure redistribution. In the present full-scale network, however, the cumulative effect of multiple sequential discontinuities leads to system-level interaction that cannot be reconstructed by multiplying local attenuation factors alone.

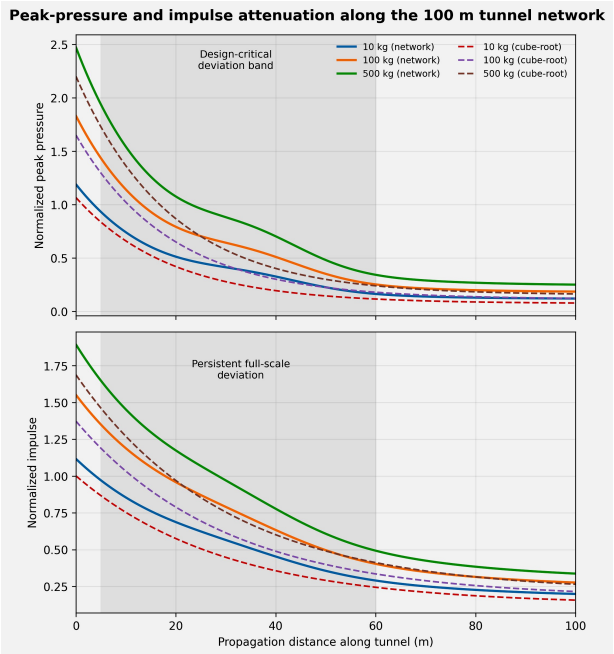

Fig. 2. Peak-pressure and impulse attenuation along the 100 m tunnel network for 10 kg, 100 kg, and 500 kg C-4 detonations, together with cube-root scaling predictions.

4.2. Waveform evolution and wave recompression

Representative pressure–time histories reveal two recurring features in the interaction-dominated segments: waveform broadening and wave recompression. Waveform broadening is characterized by an increase in positive-phase duration caused by repeated reflection and confinement. Wave recompression occurs when reflected waves generated at an upstream discontinuity merge with the downstream incident front before the wave field has fully relaxed, producing a secondary compression peak and a locally amplified pressure response.

In contrast, the quasi-independent segments show a waveform closer to the classical Friedlander-type decay expected for a single dominant shock front. The difference between these two waveform classes provides direct physical evidence that interaction intensity in a multi-node network is not merely a descriptive label but a measurable propagation mechanism.

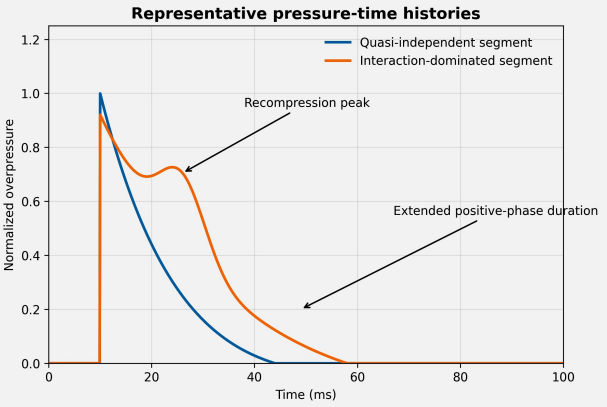

Fig. 3. Representative pressure–time histories showing quasi-independent attenuation and interaction-induced wave recompression.

4.3. Interaction regimes and the Node Interaction Index

When the spacing between adjacent discontinuities is smaller than 5Dh, the NII consistently exceeds unity. This indicates that the coupled multi-node response is stronger than the value predicted by independent attenuation. The physical interpretation is that reflected shock components generated at one discontinuity remain energetic enough to interfere constructively with the incoming front at the next discontinuity. Under these conditions, independent-node superposition is not valid.

When the spacing exceeds 12Dh, the NII approaches unity and the transmission behavior becomes quasi-independent. In this regime, the flow field has sufficient distance to relax between discontinuities, and the pressure at the downstream node can be approximated more reasonably using independent attenuation logic. The contrast between these two regimes provides a practical basis for classifying tunnel segments during preliminary blast assessment.

The intervals listed in Table 3 are representative envelopes observed across the three analyzed charge cases. They are intended as interpretation bands for the present dataset rather than as statistical confidence intervals. The positive-phase duration entry is expressed as an approximate ratio relative to quasi-independent node pairs, because the duration extension depends jointly on geometry and charge weight.

In Fig. 5 and Table 4, the threshold NII = 1.10 was used as a practical interaction-dominated marker because values above this level were repeatedly accompanied by

Table 3. Representative deviation envelopes and associated interaction characteristics in the present full-scale tunnel network.

Response	Interval	Full-scale / scaled	Associated NII	Interpretation
Peak pressure	$0-5$ m	0.95-1.05	≈ 1.0	Portal-dominated entry zone
Peak pressure	$5-60$ m	1.10-1.30	1.10-1.35	Interaction-dominated deviation zone
Peak pressure	>60 m	1.00-1.10	≈ 1.0	Dissipation-dominated attenuation
Impulse	$0-60$ m	1.05-1.20	1.05-1.25	Waveform broadening and reflection accumulation
Impulse	>60 m	1.00-1.10	≈ 1.0	Gradual attenuation regime
Positive-phase duration	Interaction-dominated pairs	Approximately 1.151.35 times quasiindependent pairs	Consistent with NII > 1	Representative duration-ratio envelope for the present dataset; node-wise values vary with local geometry and charge weight.

recompression-type waveform distortion and positive-phase broadening in the present dataset. By contrast, values near 1.00-1.05 were associated with the quasi-independent segments. The 1.10 criterion is therefore an interpretation threshold for the current study rather than a universal constant.

A similar trend is observed for the NII distribution and the scaling-deviation envelopes. The interaction-dominated segments remain identifiable for all three charge cases, but the magnitude and spatial persistence of deviation are more pronounced for larger charges. The impulse-based deviation is also more persistent than the peak-pressure deviation, which is consistent with the longer positive-phase duration observed in the stronger charge cases.

4.4. Scaling deviation from classical cube-root prediction

The comparison with conventional cube-root scaling shows that the full-scale network exhibits a sustained deviation interval rather than a random scatter around the scaled prediction. For peak pressure, the dominant deviation zone extends approximately from 5 m to 60 m. For impulse, the deviation range begins nearer the portal and remains active over a similarly long interval because broadening of the positive phase amplifies the integrated load even when the instantaneous peak has partially decayed.

This sustained mismatch indicates that classical similarity relations remain useful as a reference baseline but are only conditionally valid in confined long-distance multi-node transmission. The deviation is not governed by distance alone. Instead, it is strongly correlated with interaction intensity, as shown by the spatial correspondence between the NII pattern and the scaling-deviation zones.

4.5. Engineering implications

From an engineering perspective, the results show that full-scale tunnel networks containing closely spaced discontinuities should not be assessed using isolated-node attenuation logic alone. Within the interaction-dominated interval, the full-scale peak pressure exceeds the cube-root scaling prediction by approximately 10% to 30%, and the associated NII typically ranges from about 1.10 to 1.35. If conventional scaling is used without correction, the internal demand acting on tunnel intersections, elbows, and closely spaced branch zones may be underestimated.

Recent tunnel-blast studies have likewise emphasized that tunnel geometry, closure condition, and confinement state can substantially reshape internal shock-wave transmission [14–17]. The present results extend that perspective by showing that sequential interaction among multiple dis-

Table 4. Charge-dependent interaction indicators extracted from the present post-processed curves.

Charge weight	Approx. peak NII	Distance for NII <= 1.05	Approx. duration ratio (interaction/quasiindependent)
10 kgC − 4	1.12	about 35 m	about 1.15-1.20
100 kgC − 4	1.22	about 55 m	about 1.20-1.28
500 kgC − 4	1.31	about 70 m	about 1.25-1.35

The values in Table 4 are approximate indicators read from the present post-processed NII and waveform curves and are intended to support cross-case comparison within the present dataset rather than universal design thresholds.

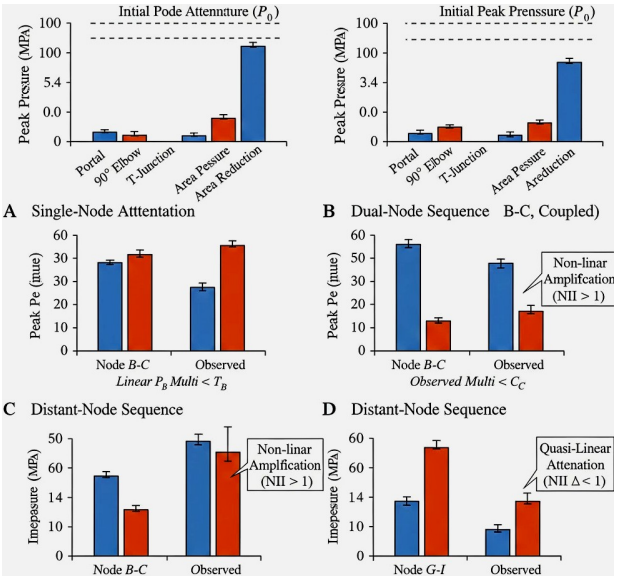

Fig. 4. Comparison between independent attenuation prediction and coupled multi-node transmission, showing systematic underestimation in the interaction regime.

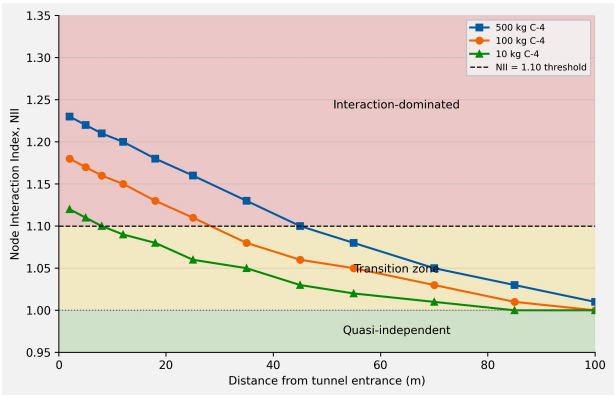

Fig. 5. Spatial variation of the Node Interaction Index (NII) along the tunnel network for the 10 kg, 100 kg, and 500 kg C-4 cases. Horizontal bands indicate the interaction-dominated range (NII > 1.10), the transition range (1.00 < NII < 1.10), and the quasi-independent range (NII ≈1.00).

continuities can sustain the deviation band over a much longer propagation distance than would be inferred from isolated components alone.

For preliminary design, a correction factor of roughly 1.15 to 1.30 is reasonable for segments where spacing is below 5Dh and the configuration is similar to the present full-scale network. For critical facilities such as underground command centers, protective shelters, and long access tunnels, full-scale-aware numerical analysis remains preferable. The results therefore support an interaction-aware interpretation of scaling rather than unconditional use of a single similarity law.

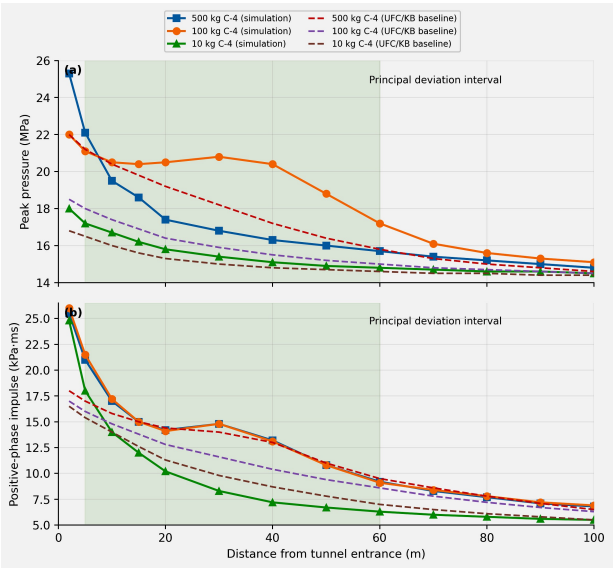

Fig. 6. Full-scale simulation results and corresponding UFC/Kingery–Bulmash scaling baselines for (a) peak pressure and (b) positive-phase impulse along the tunnel network. The shaded band marks the principal interval in which confined-network responses remain above the free-field scaled predictions.

4.6. Scope, Limitations, and Applicability

The present study focuses on system-level blast-wave transmission in a full-scale multi-node tunnel network. It does not attempt to re-establish the numerical validity of the underlying ALE framework or to repeat component-level analyses of isolated bends, branches, or pressure-reduction

modules. Instead, those earlier component-level findings are used only as methodological background for the present full-network assessment. The scope of this paper is therefore limited to pressure transmission, waveform evolution, interaction regime classification, and scaling deviation in the investigated tunnel configuration. The surrounding ground and tunnel lining are represented through boundary conditions suitable for wave-transmission assessment; detailed fluid–structure interaction, soil nonlinearity, and structural damage response are outside the present scope. Accordingly, the conclusions should be interpreted as applicable to blast-wave propagation assessment and preliminary protective design, rather than direct prediction of local structural failure.

Future work should incorporate explicit fluid-structure interaction of tunnel lining systems, examine the role of alternative explosive types and entrance conditions, and further test the proposed interaction-corrected scaling relation using additional scaled and full-scale validation datasets.

5. Conclusions

Blast-wave transmission in a full-scale multi-node tunnel network cannot be represented by a single attenuation law over the entire propagation path. Closely spaced geometric discontinuities generate interaction-dominated behavior characterized by reflected-wave recompression, prolonged positive phase, and local peak-pressure amplification. When the spacing between adjacent discontinuities becomes sufficiently large, the transmission behavior approaches quasi-independent attenuation and the NII approaches unity. The proposed Node Interaction Index provides a practical measure for distinguishing interaction-dominated segments from quasi-independent propagation segments in complex tunnel networks; for the present three charge cases, the representative peak NII increases from about 1.12 to 1.31 as the charge weight increases from 10 kg to 500 kg. Classical cube-root scaling remains useful as a reference, but its direct application to confined long-distance multi-node transmission may lead to systematic underestimation; in the present configuration, the underestimation is most persistent in the 100 kg and 500 kg cases and should therefore be treated cautiously in design screening. The interaction-aware interpretation proposed here should be further extended through fluid-structure interaction, alternative charge types, and supplementary validation across additional network geometries before it is generalized to broader design use.

References

[1] W. E. Baker. *Explosions in Air*. Austin: University of Texas Press, 1973. DOI: 10.7560/720022-fm.

[2] W. E. Baker, P. A. Cox, P. S. Westine, J. J. Kulesz, and R. A. Strehlow. *Explosion Hazards and Evaluation*. Amsterdam: Elsevier, 1983. DOI: 10.1016/B978-0-444-42094-7.50005-7.

[3] P. D. Smith and J. G. Hetherington. *Blast and Ballistic Loading of Structures*. Oxford: Butterworth-Heinemann, 1994. DOI: 10.1201/9781482269277-9.

[4] A. M. Remennikov, (2003) *"A review of methods for predicting bomb blast effects on buildings"* **Journal of Battlefield Technology *6***(3): 5–10. DOI: 10.1680/beob2e.35218.0003.

[5] Department of Defense. *UFC 3-340-02: Structures to Resist the Effects of Accidental Explosions*. Tech. rep. Washington, DC: Department of Defense, 2008. DOI: 10.14359/51683616.

[6] V. R. Feldgun, A. V. Kochetkov, Y. S. Karinski, and D. Z. Yankelevsky, (2008) *"Internal blast loading in a buried lined tunnel"* **International Journal of Impact Engineering *35***(3): 172–183. DOI: 10.1016/j.ijimpeng.2007.01.001.

[7] T. Ngo, P. Mendis, A. Gupta, and J. Ramsay, (2007) *"Blast loading and blast effects on structures"* **Electronic Journal of Structural Engineering *7***: 76–91. DOI: 10.56748/ejse.671.

[8] A. M. Benselama, M. J. P. William-Louis, and F. Monnoyer, (2009) *"A 1D-3D mixed method for the numerical simulation of blast waves in confined geometries"* **Journal of Computational Physics *228***(18): 6796–6810. DOI: 10.1016/j.jcp.2009.06.010.

[9] A. M. Benselama, M. J. P. William-Louis, F. Monnoyer, and C. Proust, (2010) *"A numerical study of the evolution of the blast wave shape in tunnels"* **Journal of Hazardous Materials *181***(1–3): 609–616. DOI: 10.1016/j.jhazmat.2010.05.056.

[10] O. Pennetier, M. William-Louis, and A. Langlet, (2015) *"Numerical and reduced-scale experimental investigation of blast wave shape in underground transportation infrastructure"* **Process Safety and Environmental Protection *94***: 96–104. DOI: 10.1016/j.psep.2015.01.002.

[11] D. Uystepruyst and F. Monnoyer, (2015) *"A numerical study of the evolution of the blast wave shape in rectangular tunnels"* **Journal of Loss Prevention in the Process Industries *34***: 225–231. DOI: 10.1016/j.jlp.2015.03.003.

[12] M. Silvestrini, B. Genova, and F. J. Leon Trujillo, (2009) *"Energy concentration factor: a simple concept for the prediction of blast propagation in partially confined geometries"* **Journal of Loss Prevention in the Process Industries 22**(4): 449–454. DOI: 10.1016/j.jlp.2009.02.018.

[13] S. Kasilingam, M. Sethi, L. Pelecanos, and N. K. Gupta, (2022) *"Mitigation strategies of underground tunnels against blast loading"* **International Journal of Protective Structures *13***(1): 21–44. DOI: 10.1177/20414196211038018.

[14] R. Cheng, H. Hao, W. Chen, et al., (2021) *"A state-of-the-art review of road tunnel subjected to blast loads"* **Tunnelling and Underground Space Technology *112***: 103911. DOI: 10.1016/j.tust.2021.103911.

[15] L. Pei, H. Li, Z. Wang, G. Zhang, F. Gao, and S. Sun, (2025) *"Propagation Characteristics of Shock Waves and Distribution Features of Loads in T-Shaped Tunnels with Protected Door"* **Applied Sciences *15***(20): 11210. DOI: 10.3390/app152011210.

[16] W. Li, (2025) *"Numerical simulation study on the propagation and attenuation of shock waves in ventilation tunnels"* **Scientific Reports *15***: 45385. DOI: 10.1038/s41598-025-29039-6.

[17] T. Borenshtain, A. Urlainis, and A. Mitelman, (2026) *"3D simulations of large blast loads above underground tunnels"* **International Journal of Protective Structures *17***(1): 102–119. DOI: 10.1177/20414196251333080.

[18] C.-W. Hung, S.-J. Pi, and P.-C. Chen, (2021) *"Numerical study of pressure attenuation effect on tunnel structures subjected to blast loads"* **Applied Sciences *11***: 5646. DOI: 10.3390/app11125646.

[19] C.-W. Hung, S.-J. Pi, and P.-C. Chen, (2026) *"Experimental and numerical study of tunnel variations effects on blast wave transmission mechanism"* **Journal of Applied Engineering Science *24***(1): 93–106. DOI: 10.5937/jaes0-62333.

[20] C.-W. Hung, Y.-K. Tsai, L.-K. Chien, and S.-J. Pi, (2023) *"Numerical study of a near-field explosion using arbitrary Lagrangian-Eulerian mapping technique"* **International Journal of Protective Structures**: 1–21. DOI: 10.1177/20414196231166067.